Turkish Journal of Earth Sciences (Turkish J. Earth Sci.), **Vol. 17**, 2008, pp. 297–315. *Copyright ©TÜBİTAK*
First published online 12 December 2007

Magma Interaction Processes Inferred from Fe-Ti Oxide Compositions in the Dölek and Sarıçiçek Plutons, Eastern Turkey

ORHAN KARSLI[1], FARUK AYDIN[2], İBRAHİM UYSAL[3] & M. BURHAN SADIKLAR[3]

[1] Karadeniz Technical University, Department of Geological Engineering, TR–29000 Gümüşhane, Turkey
(E-mail: okarsli@ktu.edu.tr)
[2] Niğde University, Department of Geological Engineering, TR–51200 Niğde, Turkey
[3] Karadeniz Technical University, Department of Geological Engineering, TR–61080 Trabzon, Turkey

Abstract: Magnetite-ulvöspinel and ilmenite-hematite solid solution intergrowths from the high-K calc-alkaline Dölek and Sarıçiçek plutons, Eastern Turkey, were investigated using microprobe analyses. Compositions of twenty-eight samples from the host rocks and their enclaves in the plutons were used to estimate the oxygen fugacity and temperature. The ilmenite and ulvöspinel component exsolves out along certain preferred crystallographic planes in the titanomagnetite of the host rocks, while they are always absent in those of the mafic microgranular enclaves. The titanomagnetite and ilmenite show variations as $Mt_{98-70}Usp_{02-30}$ and $Ilm_{99-65}Hm_{01-35}$ in composition, respectively. Estimations of oxygen fugacity and temperature using the titanomagnetite-ilmenite thermometry/oxygen barometry range from $\log fO_2$ of -15.30 to -20.48 in host rocks, $\log fO_2$ of -15.39 to -20.80 in the mafic microgranular enclaves and 617±6 to 758±23 °C in host rocks, 622±6 to 735±24 °C in the mafic microgranular enclaves, possibly indicating crystallisation temperature. Applying magnetite-ilmenite thermometry/oxygen barometry to the granitoid rocks also involves microprobe analyses of ilmenite lamellae in titanomagnetite and this method yielded mean temperatures of 679±18 °C. The specific forms and chemical properties of Fe-Ti oxides, and similarities in crystallization temperature and oxygen fugacity of the host rocks and the mafic microgranular enclaves (MME) obtained from the Fe-Ti oxide pairs imply that thermal equilibrium probably occurred between two contrasted magmas, which mixed in various proportions so that possibly a felsic and a more mafic magma interaction occurred in a convectively dynamic magma chamber during crystallization of the plutons. Probably, underplating may be responsible for genesis of the hybrid plutons. Thus, for mixing of coeval magmas derived from a lithospheric upper mantle (mafic end-member) and lower crust (felsic end-member), a thermal anomaly should be supplied. Upwelling of hot asthenospheric material results in thermal perturbation and melting of lithospheric mantle. Intrusion of hot lithospheric mantle-derived mafic magma then induced lower crustal melting, producing felsic melt. Mixing of the lower crust-derived melt and lithospheric mantle-derived magma formed the hybrid plutons. This process requires a post-collisional extensional tectonic setting during the Eocene in the Eastern Pontides.

Key Words: Dölek and Sarıçiçek plutons, Eastern Turkey, magma interaction, magnetite-ilmenite thermometry/oxygen barometry

Dölek ve Sarıçiçek Plütonlarındaki Fe-Ti Oksit Bileşimlerinde Magma Karışım İzleri, Doğu Türkiye

Özet: Doğu Türkiye'de, yüksek-K'lu kalk-alkalin Dölek ve Sarıçiçek plütonlarındaki manyetit-ulvospinel ve ilmenit-hematit katı ergiyik ürünleri mikroprop analizleri ile incelenmiştir. Oksijen kısmi basıncı ve sıcaklık tahminleri için, plütonlarda anklav ve ana kayaçlardan toplanan yirmi sekiz örneğin bileşimleri kullanılmıştır. İlmenit ve ulvöspinel, ana kayaçlardaki titanomanyetitlerde bazı kristalografik yüzeyler boyunca düzenli bir biçimde ayrılım lamelleri halinde oluşmuşlardır. Ancak, bu oluşum, mafik mikrogranular enklavların titanomanyetitlerinde bulunmamaktadır. Titanomanyetit ve ilmenit sırasıyla, $Mt_{98-70}Usp_{02-30}$ ve $Ilm_{99-65}Hm_{01-35}$ bileşimindedir. Titanomanyetit-ilmenit termometre/oksijen barometresi kullanılarak elde edilen oksijen fugasitesi tahminleri, ana kayaçlarda -15.30 $\log fO_2$ ila -20.48 $\log fO_2$ arasında, mafik mikrogranular enklavlarda -15.39 $\log fO_2$ ila -20.80 $\log fO_2$ arasındadır. Sıcaklık tahminleri ise, ana kayaçlarda; 617 ± 6 ila 758±23 °C arasında, mafik mikrogranular enklavlarda ise 622±6 ile 735±24 °C arasındadır. Sıcaklık değerleri, yüksek olasılıkla kristalleşme sırasındaki değerlerini temsil ederler. Granitoyid kayaçlar üzerinde yapılan bu titanomanyetit-ilmenit jeotermometresi, lamel biçimli ilmenit çiftleri üzerinde de denenmiştir ve ortalama 679±18 °C oluşum sıcaklığı belirlenmiştir. Fe-Ti oksitlerin spesifik kristal biçimleri, kimyasal özellikleri ve ana kayaç ve mafik mikrogranular anklavlardan (MME) alınan Fe-Ti oksit

çiftlerinden hasaplanan sıcaklık ve oksijen fugasitesi değerlerindeki benzerlikler, bu plütonların kristalizasyonu süresince, dinamik bir magma odasında muhtemelen bir felsik ile bir mafik magmanın çeşitli oranlarda karışmış olabileceğini ve bu iki tezat magma arasında yüksek olasılıkla termal dengenin sağlanmış olabileceğine işaret etmektedir. Hibrit plütonların oluşumlarında, büyük olasılıkla, yükselen sıcak magmanın manto-kabuk sınırına yerleşerek magma odası oluşturması mekanizması etkili olmuştur. Litosferik üst manto (mafik uç üye) ve alt kabuktan (felsik uç üye) türeyen eşyaşlı magmaların karışabilme modelinin gerçekleşebilmesi için sıcaklık kaynağının tanımlanması gerekir. Sıcak astenosferin yükselmesi neticesinde, sıcaklık değişimi meydana gelir ve litosferik manto ergimiş olabilir. Daha sonra, litosferik mantodan türeyen sıcak magma alt kabuğu ergitir ve felsik magma meydana gelir. Alt kabuk ve üst manto kaynaklı magmaların karışımı bu hibrit plütonları oluşturmuştur. Bu olay Doğu Pontidler'de Eosen sürecinde, çarpışma sonrası genişlemeli bir tektonik ortamın varlığını gerektirir.

Anahtar Sözcükler: Dölek ve Sarıçiçek plütonları, Doğu Türkiye, magma etkileşimi, manyetit-ilmenit termometresi/oksijen barometresi

Introduction

Despite recent advances in understanding magmatic processes through geochemical and isotopic signatures, hybrid granitoids are perhaps the least understood, in terms of magma processes and genesis. Iron-titanium oxide minerals, as small parts of the hybrid granitoids, are useful for studying the crystallization conditions of hybrid granitoid systems. They may also provide evidence for magma interactions in a magma chamber because their compositions change much faster than those of silicates during temperature fluctuation that may be caused by magma mixing. Indeed, they are fast enough to record changes in magma chamber temperature (e.g., Nakamura 1995; Venezky & Rutherford 1999; Devine *et al.* 2003) and are sensitive indicators of magma interactions between two-contrasting magmas. Also, the oxygen fugacity of the granitoid rocks directly determines the stability of, and the Fe content of Fe-Mg silicate minerals as well as the stability of common oxide phases such as magnetite, ilmenite and rutile. The latter has a direct influence on the degree of solid solution between either magnetite and ulvöspinel or between ilmenite and hematite (e.g., Frost *et al.* 1988; Lindsley *et al.* 1990; Andersen *et al.* 1991; Harlov 1992, 2000). Thus, the oxygen fugacity and corresponding temperature for granitoid rocks may be ascertained, if they contain coexisting assemblages of magnetite-ilmenite (e.g., Spencer & Lindsley 1981; Andersen *et al.* 1991; Frost & Lindsley 1991). This thermometry/oxygen barometry is very commonly applied to igneous rocks to describe their petrological characters (Frost & Lindsley 1991; Ghiorso & Sack 1991).

In this study, we examine iron-titanium oxides in samples from the hybrid Dölek and Sarıçiçek plutons with back-scattered electron (BSE) images and try to determine the chemical compositions of the oxides with an electron microprobe analyzer. In addition, this paper uses Fe-Ti oxides as a geothermobarometer to constrain the magma interactions controlling the generation of these hybrid granitoids. The rationale is to monitor the lamellae in titanomagnetite of the host rocks to try to detect whether or not felsic magma in the system could be heated by mantle-derived mafic magma. It also tries to determine a possible geodynamic system in which the hybrid plutons occurred.

Regional Geology

The Eastern Pontides are generally divided into a northern and a southern zone, based on the differences between the rock associations (Akın 1979; Okay & Şahintürk 1997; Okay *et al.* 1997). The initiation of arc magmatism (Late Cretaceous–Late Paleocene) is related to northward subduction of the northern branch of Neotethys in the Eastern Pontides (e.g., Akın 1979; Şengör & Yılmaz 1981; Okay & Şahintürk 1997; Yılmaz *et al.* 1997; Şengör *et al.* 2003; Yılmaz & Kandemir 2006) and the subsequent collision between the Pontides and the Tauride-Anatolide platform, although the timing of the collision is still controversial (e.g., Robinson *et al.* 1995; Okay & Şahintürk 1997; Şen *et al.* 1998; Şengör *et al.* 2003). Okay *et al.* (1997) suggested that the collision occurred during the Late Paleocene to Early Eocene, based on field relationships and ages of granitoids. Also, Boztuğ *et al.* (2004) reported apatite fission-track data indicating a Late Paleocene to Early Eocene collision between the Eurasian plate and the Tauride-Anatolide platform. The basement of the Eastern Pontides consists of Devonian metamorphic rocks, Lower Carboniferous granitic and dacitic rocks, Upper Carboniferous–Lower Permian shallow-marine to

terrigenous sedimentary rocks and Permo–Triassic metabasalt, phyllite and marble (e.g., Yılmaz 1972; Şengör & Yılmaz 1981; Okay & Şahintürk 1997; Yılmaz *et al.* 1997). The basement is overlain by Lower–Middle Jurassic tuffs, interbedded pyroclastic and clastic sedimentary rocks, and Upper Jurassic–Lower Cretaceous carbonates (Şengör & Yılmaz 1981; Okay & Şahintürk 1997). The upper Mesozoic and Lower Cenozoic are represented by ophiolitic mélange, volcanic rocks and granitoid plutons (e.g., Tokel 1977; Yılmaz & Boztuğ 1996; Boztuğ *et al.* 2004); they are covered by Upper Paleocene–Lower Eocene foreland flysch and post-Eocene terrigenous sediments (e.g., Okay & Şahintürk 1997).

The Eastern Pontides extend for 450 km along the northeastern coast of Turkey (Figure 1a, b) and include a series of granitoid bodies, which are parts of the composite Kaçkar Batholith (Boztuğ *et al.* 2006), emplaced during Early Cretaceous to Late Eocene times. The granitoid bodies occurred in various geodynamic settings and have different ages (Taner 1977; Moore *et al.* 1980; Boztuğ & Harlavan 2007; Boztuğ *et al.* 2007) and compositions (Yılmaz & Boztuğ 1996; Karslı *et al.* 2002; Topuz *et al.* 2005; Boztuğ *et al.* 2006; Dokuz *et al.* 2006; Topuz & Okay 2006). The compositions of the plutons in the Eastern Pontides vary from low-K tholeiitic through calc-alkaline (rarely high-K) metaluminous granitoids and peraluminous leucogranites to alkaline syenites and monzonites (e.g., Karslı *et al.* 2002; Şahin *et al.* 2004; Boztuğ *et al.* 2006). Their emplacement took place during crustal thickening related to the arc-continent collision and subsequent post-collisional extension (e.g., Yılmaz & Boztuğ 1996; Karslı *et al.* 2004a, b, 2007; Topuz *et al.* 2005; Boztuğ & Harlavan 2007; Boztuğ *et al.* 2007).

Geology of the Dölek and Sarıçiçek Plutons

The Dölek and Sarıçiçek plutons are part of the composite E–W-trending Kaçkar Batholith, intruded between 30 and 80 Ma ago (Taner 1977; Moore *et al.* 1980; Boztuğ & Harlavan 2007; Boztuğ *et al.* 2007), in the Eastern Pontides of Eastern Turkey. The Dölek and Sarıçiçek plutons are located in the southern part of the Eastern Pontides (Figure 1b). Both plutons are elliptical; the long axis of the Dölek pluton extends NW–SE, while that of the Sarıçiçek pluton trends NE–SW. They cover an area of <40 km^2 and have a wide contact aureole in Early Eocene andesitic rocks of the Alibaba Formation (Figure 2). All contacts with the country rocks are sharp. Country rock xenoliths are absent. The host rocks of the plutons are undeformed and no shear zones were observed. The plutons have a biotite K-Ar cooling age of 44–42 Ma (Karslı *et al.* 2007).

Sampling and Analytical Procedure

Fresh samples were collected from outcrops of the Dölek and Sarıçiçek plutons (Figure 2). Selected samples of both the host rocks and mafic microgranular enclaves (MMEs) were homogeneously obtained from all over the plutons. Seventy-seven oxide pairs in the host rock and MMEs were obtained for thermobarometric determinations. Compositions of iron-titanium oxides and accompanying silicates were determined using the CAMECA-SX 51 electron microprobe equipped with five wavelength-dispersive spectrometers in the Mineralogical Institute of Heidelberg University, Germany. Synthetic and natural oxides and silicates were used for calibration. The correction procedures were performed using CAMECA's PAP algorithm of Pouchou & Pichoir (1985). Operating conditions were 15 kV accelerating voltage and 20 nA beam current. Counting time was usually 10 s for major elements, i.e., Si, Al, Fe, Ca, Na and K. The analyses were performed with a beam diameter of 1 μm except for feldspars analyzed with a defocused beam (10 μm) in order to minimize possible alkaline diffusion. Fe^{3+} was estimated assuming charge balance and ideal mineral stoichiometries. Detection limits were 0.03 wt% SiO_2, 0.06 wt% TiO_2, 0.06 wt% Al_2O_3, 0.07 wt% Cr_2O_3, 0.10 wt% FeO, 0.08 wt% MnO, 0.07 wt% MgO, 0.04 wt% CaO, 0.04 wt% Na_2O and 0.03 wt% K_2O.

Mineralogy and Petrography of the Dölek and Sarıçiçek Plutons

Host Rocks

The Dölek and Sarıçiçek plutons form outcrops less than 10 km long and up to 4 km wide (Figure 2). They comprise a variety of granitoid rocks including granite, granodiorite, tonalite, monzonite and diorite, with granodiorite and tonalite dominant (~70% of the mass volume). All the rock units from both plutons share several common petrographic and geochemical features and they are therefore described together here. In both

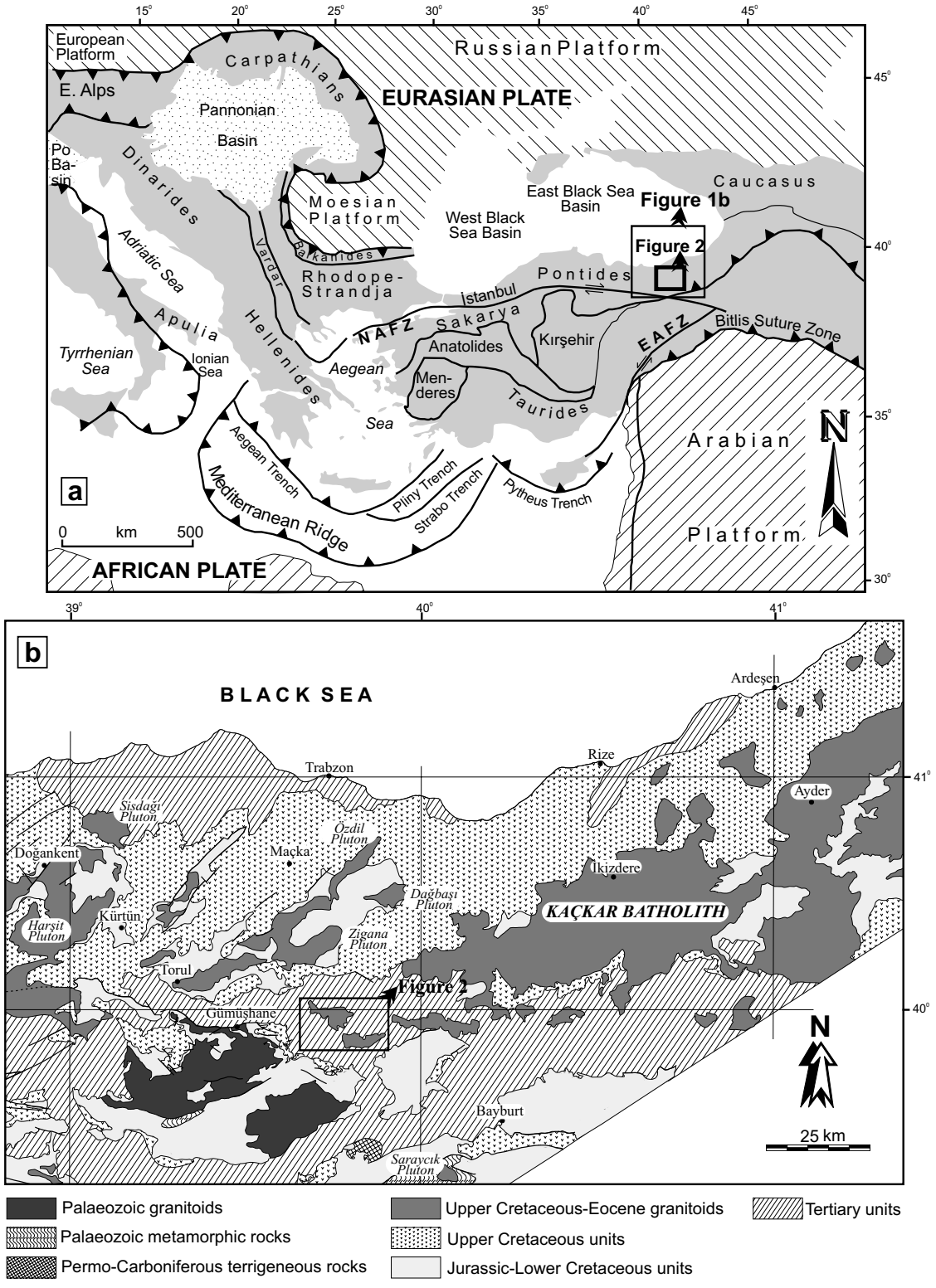

Figure 1. (a) A map showing the major blocks of Turkey. (b) Simplified geological map of the Eastern Pontides (modified from Gedik *et al.* 1992).

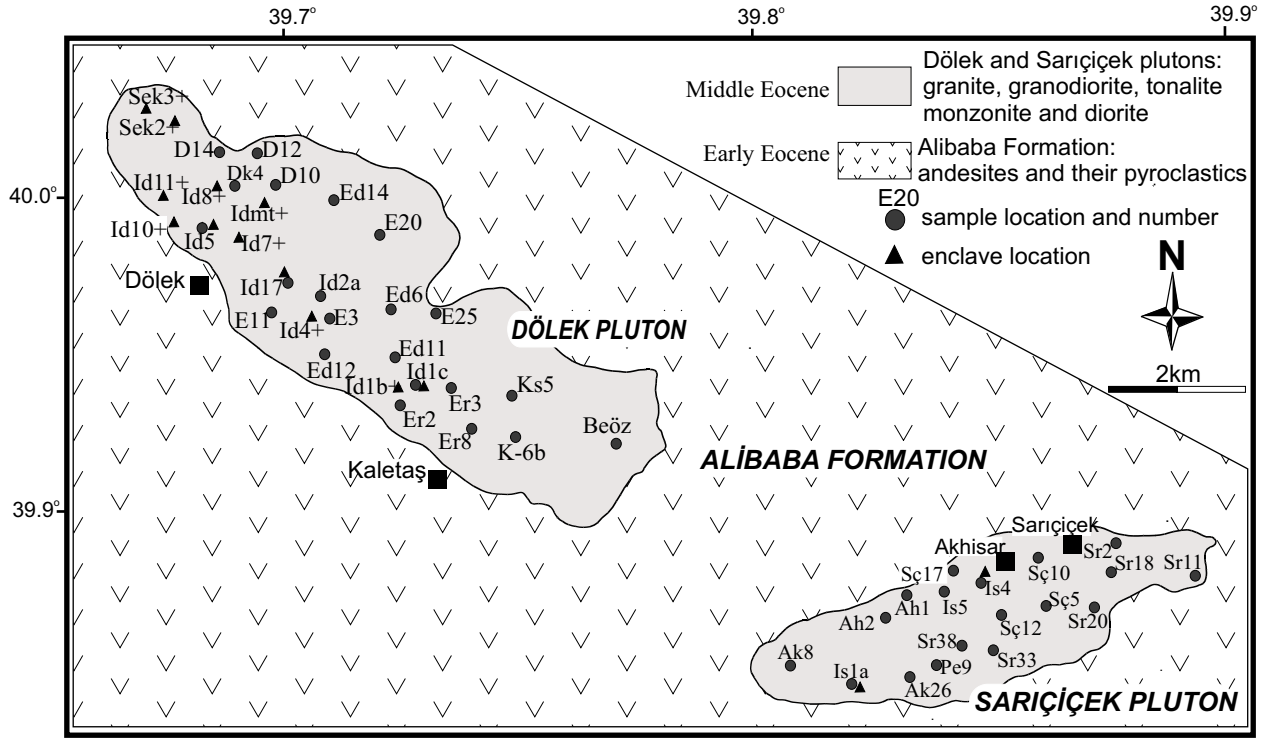

Figure 2. Geological map of the Dölek and Sarıçiçek Plutons (modified from Karslı *et al.* 2007).

plutons monzonite and diorite never exceed 25%, and granite occupies less than 10% of the total volume. The contacts between all lithotypes are transitional. The main rocks of the plutons are medium-grained (Figure 3a–c). Plagioclase grains displaying oscillatory zoning (~10 mm; Figure 3d) can be attributed to magma mixing (e.g., Vernon 1990; Hibbard 1991; Waight *et al.* 2000). They usually occur in a fine-grained matrix of plagioclase (25–73%), K-feldspar (9–42%), quartz (4–35%), amphibole (1–20%), biotite (0–17%), pyroxene (cpx; 0–10%) and iron-titanium oxides (1–7%). Mafic constituents are mainly represented by amphibole, biotite and pyroxene. Dioritic and monzonitic rocks contain more abundant amphibole and biotite (amphibole > biotite) than in granitic, granodioritic and tonalitic rocks. Pyroxene occurs only in dioritic rocks. Lath-shaped plagioclase is common, and ranges in composition from An_{64} to An_{25}, with Or content rarely exceeding 1 mol. %. Oscillation controlled by An mol. % variation changes from 10 to 150 mm in thickness and has ~15 mol. % An variation. Orthoclase ($Or_{96-74}Ab_{3-26}An_{1-0}$) contains inclusions of finer-grained plagioclase, amphibole and biotite. Quartz is anhedral and poikilitic and also encloses K-feldspar. Green to brownish green amphiboles are generally calcic and characterized by X_{Mg} [=Mg/(Mg+Fe_{tot})]= 0.51–0.82. Biotite forms large subhedral to euhedral crystals (10–15 mm in length) with inclusions of Fe-Ti oxide and apatite (Figure 3e) and has variable TiO_2 content (3.36–6.50 wt%) and X_{Mg} of 0.53 to 0.73 (Table 1). Bladed biotite was also observed in the host rocks (Figure 3d). Pyroxene occurs as small, yellowish green subhedral grains (~1 mm) (Figure 3e). Diopsidic, salitic and augitic pyroxenes have X_{Mg} ranging from 0.66 to 0.78. Fe-Ti oxides coexist with mafic silicates (Figure 3e). Large titanomagnetite ($Mt_{98-70}Usp_{30-02}$) crystals surrounded by finer-grained ilmenite ($Ilm_{99-65}Hm_{35-01}$) show well-developed exsolution lamellae. Apatite exists as irregular blobs within titanomagnetite, biotite, amphibole and plagioclase. Titanite is concentrated around large titanomagnetite crystals, but may also form aggregates of twinned crystals. Prismatic zircon is an accessory phase in all rock types in these plutons.

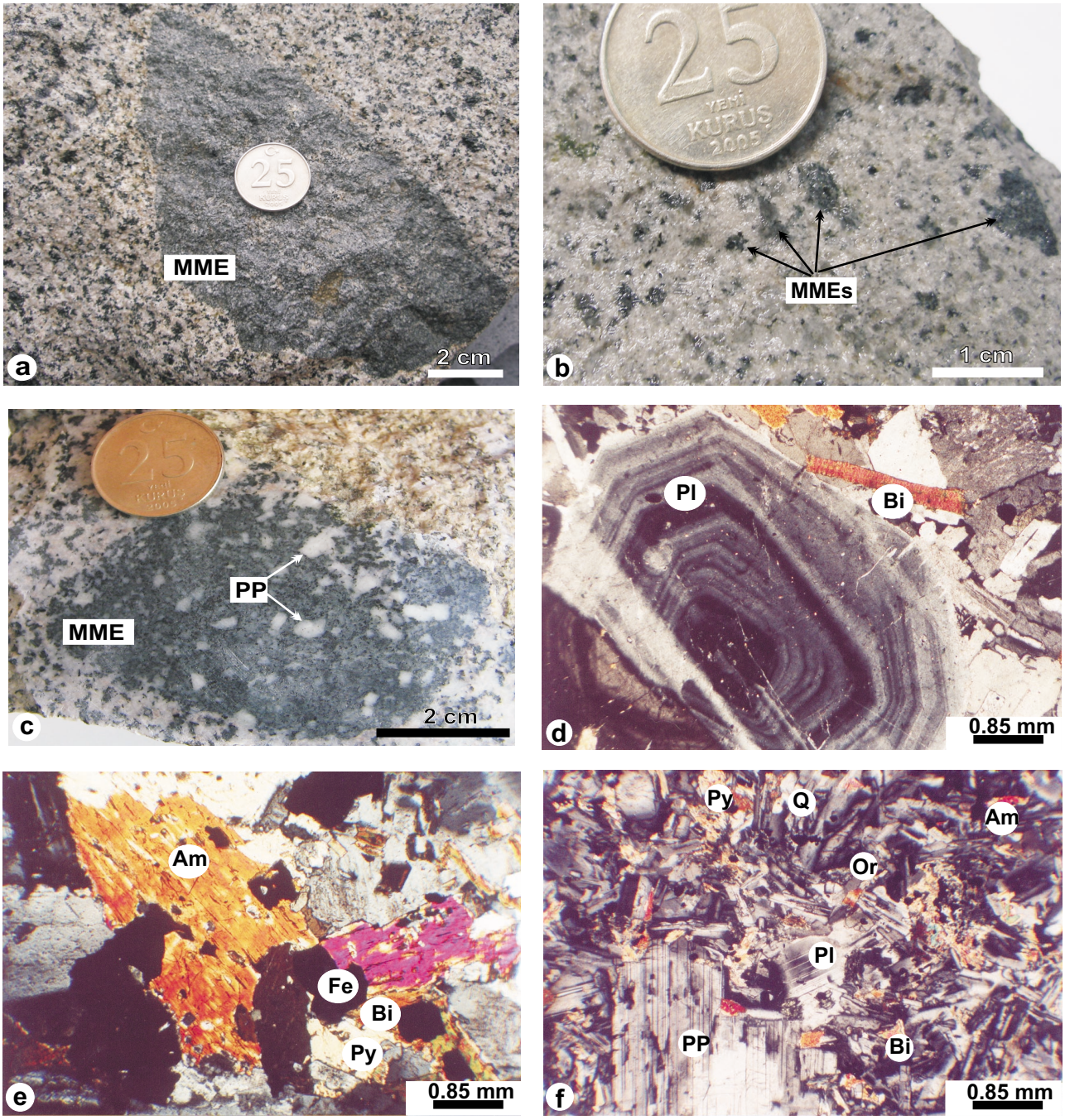

Figure 3. (a–c) Macroscopic view of the MMEs within the host rocks and (d–f) photomicrograph showing textural relationships of the host granitoid rocks and their enclaves. The features are amphibole (Am), plagioclase (Pl), biotite (Bi), orthoclase (Or), quartz (Q), pyroxene (Py), Fe-Ti oxides (Fe) and plagioclase phenocryst (PP).

Mafic Microgranular Enclaves

The MMEs are widespread within the plutons, but their spatial distribution is heterogeneous, and mainly concentrated in the more felsic rocks. Compared to the host rocks, the MMEs are fine-grained, and gabbroic diorite, diorite and quartz monzodiorite in composition. They have ellipsoidal and flattened shapes. These features suggest plastic behavior when they were incorporated

Table 1. The representative chemical compositions of the investigated iron-titanium oxide minerals

Mineral	Ilm-gr	Mt	Mt	Ilm-la	Ilm-gr	Mt	Ilm-la	Mt	Ilm-gr	Mt	Ilm-la	Mt	Ilm-gr	Mt	Mt	Mt	Mt	Ilm-gr	Mt	Ilm-la
Sample/	Be-2	Be-2	Be-3	Be-3	Is1-2	Is1-2	Is1-4	Is1-4	D12-1	D12-1	D12-4	D12-4	Id4-1	Id4-1	Id4-1	Id4-2	Is4-2	Id17-2	Id17-2	Id11-2
Probe no	23	24	28	29	4	5	7	10	37	44	40	45	6	9	9	11	3	3	4	14
SiO_2	0.01	0.02	0.03	0.08	0.01	0.03	0.02	0.06	0.12	0	0.02	0.03	0.05	0	0	0.03	0.09	0.04	0.02	0
TiO_2	48.73	0.53	1.43	48.94	48.09	1.83	48.6	2.35	49.1	0.31	48.1	0.17	48.04	0.37	0.37	5.1	1.72	48.32	0.7	46.97
Al_2O_3	0	0.3	0.34	0	0	0.46	0	0.66	0	0.08	0	0.05	0	0.35	0.35	0.28	1.71	0	0.11	0
Fe_2O_3	6.62	68.29	66.05	7.08	8.7	64.79	7.21	63.15	8.49	69.63	9.38	69.84	7.59	67.73	67.73	58.8	62.98	7.99	68.18	11.32
FeO	34.69	31.72	32.23	36.07	38.46	32.56	39.25	32.86	38.58	31.65	37.53	31.69	36.87	31.28	31.28	35.16	32.21	36.62	31.75	35.68
MnO	8.83	0.05	0.27	7.33	4.5	0.23	4.13	0.3	5.28	0.15	5.36	0.06	5.76	0.08	0.08	0.52	0.28	5.5	0.1	6.33
MgO	0.08	0.04	0.06	0.32	0.09	0.03	0.1	0.03	0.1	0.01	0.08	0	0.05	0	0	0.02	0.11	0.3	0.02	0.05
Total	98.96	100.95	100.41	99.82	99.83	99.73	99.31	99.41	101.67	101.83	100.2	101.84	98.36	99.81	99.81	99.91	99.1	98.77	100.88	100.35
Cations on the basis of 4 oxygens (magnetite) and 3 oxygens (ilmenite)																				
Si	0	0.001	0.001	0.002	0	0.001	0.001	0.002	0.003	0	0.001	0.001	0.001	0	0	0.001	0.003	0.001	0.001	0
Ti	0.937	0.015	0.041	0.931	0.918	0.053	0.932	0.068	0.919	0.009	0.912	0.005	0.93	0.011	0.011	0.147	0.05	0.93	0.02	0.893
Al	0	0.013	0.015	0	0	0.021	0	0.03	0	0.004	0	0.002	0	0.016	0.016	0.013	0.077	0	0.005	0
Fe^{3+}	0.126	1.955	1.9	0.134	0.164	1.871	0.136	1.829	0.155	1.979	0.174	1.986	0.137	1.963	1.963	1.691	1.816	0.137	1.953	0.214
Fe^{2+}	0.743	1.012	1.03	0.764	0.818	1.045	0.839	1.059	0.807	1.003	0.795	1.004	0.804	1.008	1.008	1.13	1.038	0.801	1.016	0.755
Mn	0.191	0.002	0.009	0.157	0.097	0.007	0.089	0.01	0.111	0.005	0.115	0.002	0.126	0.003	0.003	0.017	0.009	0.119	0.003	0.136
Mg	0.003	0.002	0.003	0.012	0.003	0.002	0.004	0.002	0.004	0.001	0.003	0	0.002	0	0	0.001	0.006	0.011	0.001	0.002
Total	2	3	3	2	2	3	2	3	2	3	2	3	2	3	3	3	3	2	3	2

Mineral	Ilm-la	Mt	Mt	Ilm-la	Mt	Ilm-gr	Ilm-la	Mt	Usp	Usp	Ilm-lt	Ilm-lt	Ilm-gr	Mt	Ilm-gr	Mt	Mt	Ilm-la	Ilm-gr	Mt
Sample/	Id11-2	Id11-2	Ah2-3	Ah2-3	Ah2-2	Ah2-2	Sek5	Sek5	Sek5	Sek5	D20	D20	Sr20	Sr20	Sr20	Sr20	Sr12	Sr12	Id17*	Id17*
Probe no	14	15	4	5	7	8	5	6	15	17	7	8	33	36	32	35	36	39	5	8
SiO_2	0	0.02	0.04	0.01	0.03	0	0.03	0	0.04	0.05	0.02	0.01	0.09	0.06	0.06	0.04	0.04	0.02	0.02	0.02
TiO_2	46.97	2.46	4.23	47.72	6.1	48.29	48.05	4.09	21.49	15.55	49.07	49.65	47	0.62	46.57	0.7	3.17	45.55	49.06	0.29
Al_2O_3	0	0.37	0.62	0	1.53	0	0	0.39	0	0.05	0	0	0	0.03	0	0.12	0.15	0	0	0.07
Fe_2O_3	11.32	63.29	59.97	10.04	54.75	9.49	8.16	60.04	56.86	69.13	7.47	6.1	10.48	67.85	11.46	67.42	62.85	13.1	5.64	68.63
FeO	35.68	32.66	34.47	38.61	35.82	37.32	33.04	33.89	19.3	13.87	31.14	34.77	36.81	31.57	36.54	31.57	33.72	34.54	37.59	31.3
MnO	6.33	0.47	0.46	4.04	0.82	5.62	9.32	0.5	0.01	0.1	12.43	9.51	4.99	0.11	5.02	0.07	0.4	6.06	5.61	0.07
MgO	0.05	0.01	0.03	0.11	0.06	0.11	0.11	0.03	0	0.03	0	0.04	0.12	0	0.06	0.03	0.02	0.09	0.2	0.02
Total	100.35	99.29	99.82	100.53	99.11	100.83	98.71	98.94	97.7	98.78	100.13	100.08	99.49	100.24	99.71	99.95	100.2	99.36	98.12	100.4

Table 1. (Continued)

Cations on the basis of 4 oxygens (magnetite) and 3 oxygens (ilmenite)																				
Si	0	0.001	0.002	0	0.001	0	0.001	0	0.001	0.001	0.001	0	0.002	0.002	0.002	0.002	0.002	0.001	0.001	0.001
Ti	0.893	0.071	0.122	0.905	0.176	0.913	0.927	0.119	0.43	0.31	0.933	0.944	0.9	0.018	0.891	0.02	0.091	0.875	0.95	0.008
Al	0	0.017	0.028	0	0.069	0	0	0.018	0	0.002	0	0	0	0.001	0	0.005	0.007	0	0	0.003
Fe^{3+}	0.214	1.839	1.725	0.19	1.577	0.175	0.145	1.744	1.138	1.377	0.133	0.112	0.195	1.958	0.215	1.951	1.808	0.249	0.098	1.979
Fe^{2+}	0.755	1.056	1.107	0.815	1.147	0.789	0.721	1.101	0.431	0.307	0.667	0.739	0.79	1.017	0.782	1.018	1.079	0.741	0.821	1.006
Mn	0.136	0.015	0.015	0.086	0.027	0.12	0.202	0.016	0	0.002	0.266	0.204	0.108	0.004	0.108	0.002	0.013	0.131	0.122	0.002
Mg	0.002	0.001	0.002	0.004	0.003	0.004	0.004	0.002	0	0.001	0	0.002	0.005	0	0.002	0.002	0.001	0.003	0.008	0.001
Total	2	3	3	2	3	2	2	3	2	2	2	2	2	3	2	3	3	2	2	3
Mineral	Ilm-gr	Mt	Mt	Ilm-gr	Ilm-gr	Mt	Ilm-gr	Mt	Ilm-gr	Mt	Mt	Ilm-gr	Mt	Mt	Mt	Ilm-gr	Mt	Mt	Usp	Usp
Sample/	Is1*	Is1*	Is1*	Is1*	Id11*	Id11*	Id11*	Id11*	Id1c*	Id1c*	Sek3*	Sek3*	Sek3*	Id5*	Id4*	Id4*	Id4*	Id4*	Is4*	Id5*
Probe no	1	4	5	6	9	10	11	12	20	22	11	13	16	12	8	9	17	18	7	15
SiO_2	0.02	0.06	0.03	0.03	0.01	0.06	0.02	0.03	0	0	0.05	0.05	0.04	0.02	0.02	0.01	0	0.03	0.04	0.04
TiO_2	48.58	0.52	3.1	47.87	45.21	1.07	45.29	0.29	44.51	0.28	0.31	45.14	5.88	0.09	0.58	35.66	0.4	0.99	18.95	21.49
Al_2O_3	0	0.72	1.07	0	0	0.17	0	0.12	0	0.17	0.14	0	0.16	0.04	0.38	3.87	0.22	0.6	1.45	0
Fe_2O_3	5.97	66.38	61.33	7.75	12.97	66.48	12.87	67.8	14.15	66.85	67.59	17.78	56.18	68.3	66.55	28.79	67.62	65.82	31.01	56.86
FeO	39.59	31.34	33.15	37.05	34.42	31.78	34.72	30.97	36.11	30.63	30.91	36.02	35.93	30.79	31.17	29.86	31.17	31.68	44.55	20.3
MnO	3.87	0.06	0.33	5.5	5.97	0.16	5.76	0.07	3.32	0.04	0.1	0.1	0.01	0.02	0.06	0.33	0.02	0.03	2.24	0.01
MgO	0.09	0.01	0.09	0.1	0.05	0.03	0.06	0	0.29	0.03	0.01	0.01	0	0.02	0.01	0.01	0	0.04	0.12	0
Total	98.12	99.09	99.12	98.3	98.63	99.75	98.72	99.28	98.38	98	99.21	99.1	98.2	99.28	98.76	98.53	99.43	99.19	98.36	98.7
Cations on the basis of 4 oxygens (magnetite) and 3 oxygens (ilmenite)																				
Si	0.001	0.002	0.001	0.001	0	0.002	0.001	0.001	0	0	0.002	0.001	0.002	0.001	0.001	0	0	0.001	0.001	0.001
Ti	0.942	0.015	0.09	0.927	0.875	0.031	0.876	0.008	0.863	0.008	0.009	0.875	0.172	0.003	0.017	0.685	0.012	0.029	0.362	0.425
Al	0	0.033	0.049	0	0	0.008	0	0.005	0	0.008	0.006	0	0.007	0.002	0.017	0.116	0.01	0.027	0.043	0
Fe^{3+}	0.115	1.932	1.77	0.144	0.249	1.926	0.247	1.975	0.274	1.976	1.972	0.248	1.645	1.991	1.947	0.513	1.967	1.913	1.23	1.147
Fe^{2+}	0.855	1.015	1.075	0.804	0.743	1.026	0.749	1.007	0.779	1.005	1.007	0.874	1.174	1.002	1.015	0.678	1.011	1.027	0.311	0.426
Mn	0.085	0.002	0.011	0.12	0.13	0.005	0.125	0.002	0.073	0.001	0.003	0.002	0	0.001	0.002	0.007	0.001	0.001	0.048	0
Mg	0.003	0.001	0.005	0.004	0.002	0.002	0.002	0	0.011	0.002	0.001	0	0	0.001	0.001	0	0	0.002	0.005	0
Total	2	3	3	2	2	3	2	3	2	3	3	2	3	3	3	2	3	3	2	2

Note: Mt: Magnetite, Ilm-gr: Ilmenite grain, Ilm-la: Ilmenite lamella, *: Enclave iron-titanium oxides, Ilm-lt: Ilmenite lath

Fe_2O_3 and FeO concentrations are calculated assuming spinel stoichiometry

into the hybrid host magma (e.g., Frost & Mahood 1987; Poli & Tommasini 1991). The MMEs are commonly 1 mm to 30 cm across (Figure 3a–c). Larger MMEs never occur in the plutons. The contact with their host is usually sharp, rounded or irregular, but diffusive contacts are also observed. This morphology is attributed to a mixing of mafic and felsic magmas (e.g., Perugini *et al.* 2004). The degree of thermal, rheological and compositional contrast of co-existing mafic and felsic magmas governs the hybridization levels preserving the megascopic features of the magma mixing (e.g., Kumar *et al.* 2004). The MMEs show no cumulate textures: their magmatic textures are similar to poikilitic-equigranular textures of basic igneous rocks. The MMEs contain higher ferromagnesian phases and plagioclase and lower quartz and K-feldspar than those of the host rocks. They are composed of plagioclase (56–76%), amphibole (6–20%), biotite (1–8%), pyroxene (1–7%), orthoclase (3–7%), quartz (2–8%) and Fe-Ti oxides (2–4%); they also contain rounded and large plagioclases, which are compositionally similar to those in the host rocks (Karslı *et al.* 2007; Figure 3c, f). In some cases, the large plagioclases cross-cut the enclave/host boundary. These features, common in the enclaves worldwide, are considered to prove that the enclaves were in a liquid state when they were incorporated into the more felsic magma (e.g., Vernon 1984; Perugini *et al.* 2003). Titanomagnetite is always present and the rimming titanite is observed less frequently. Small ilmenites and acicular apatites also occur as accessories. The presence of acicular apatite and quartz ocelli reflect on the hybridization process associated with the generation of the MMEs. The mineral assemblage and mineral compositions of mafic enclaves are similar to those in the host rocks.

Results

Iron-Titanium Oxide Mineralogy

The iron-titanium oxides (titanomagnetite and ilmenite) reported here were collected from the Dölek and Sarıçiçek plutons. They usually form euhedral to anhedral crystals and exist near and within the mafic silicates such as biotite, amphibole and pyroxene (Figure 3e). Some are also surrounded by quartz, plagioclase and K-feldspar. Apatite occurs as irregular blobs within titanomagnetite crystals, which do not contain exsolution lamellae. The rimming of ilmenite by secondary titanite, implying alteration of ilmenite, was rarely observed. Ilmenites are often concentrated around the large titanomagnetites. The titanomagnetites show a well-developed exsolution lamellae, which are mainly cloth-textured, and comprise ilmenite lamellae (Figure 4a). In contrast to titanomagnetites, ilmenites do not contain hematite in varying stages of exsolution lamellae. Also, ilmenite grains do not exist as irregular blobs within titanomagnetite. Lamellae of ilmenite are sharply tapered (Figure 4e). Small-scale ilmenite-rich lamellae 1 to 5 μm wide are abundant in host rock titanomagnetites. Lamellae framework commonly develops across all the grain, with lamellae cross-cutting at 120–60° angles, arranged in a trellis pattern along the [111] lattice planes in the titanomagnetite host (Figure 4a). Some broad exsolution laths (always ilmenite) between 30 and 50 mm wide with irregular sides cross-cut the large titanomagnetites (Figure 4b) and terminate at edges parallel to the titanomagnetite grain boundaries. Euhedral titanomagnetite crystals surrounded by small euhedral ilmenites are weakly lamellized (Figure 4c). Such ilmenite exsolution textures suggest rapid cooling of magmas, probably caused by the interaction between magmas of contrasting temperature have been previously described by a number of workers (e.g., Lindsley 1981; Hammond & Taylor 1982; Haggerty 1991; Harlov 2000). Consequently, formation of titanomagnetite lamellae in the host rocks is a common microtextural feature. In contrast to the host rocks, exsolution lamellae are always absent from titanomagnetites in MMEs (Figure 4d).

Iron-Titanium Oxide Composition

Selected oxide compositions of representative samples are given in Table 1. The studied titanomagnetites have compositions between $Mt_{70}Usp_{30}$ and $Mt_{98}Usp_{02}$, and the ilmenites usually coexisting with titanomagnetite range from $Ilm_{99}Hm_{01}$ to $Ilm_{65}Hm_{35}$ (Figure 5). The MnO and MgO contents of titanomagnetites are low and vary from 0.01 to 0.82 wt% and 0.01 to 0.11 wt%, respectively. Titanomagnetites have variable Al_2O_3 contents (0.03–1.53 wt%). In contrast to the titanomagnetite, euhedral ilmenites coexisting with titanomagnetite have high MnO contents (3.32–9.32 wt%) and low MgO contents (0.01–0.05 wt%). The MnO concentration in lath-shaped ilmenite is much higher than in the other

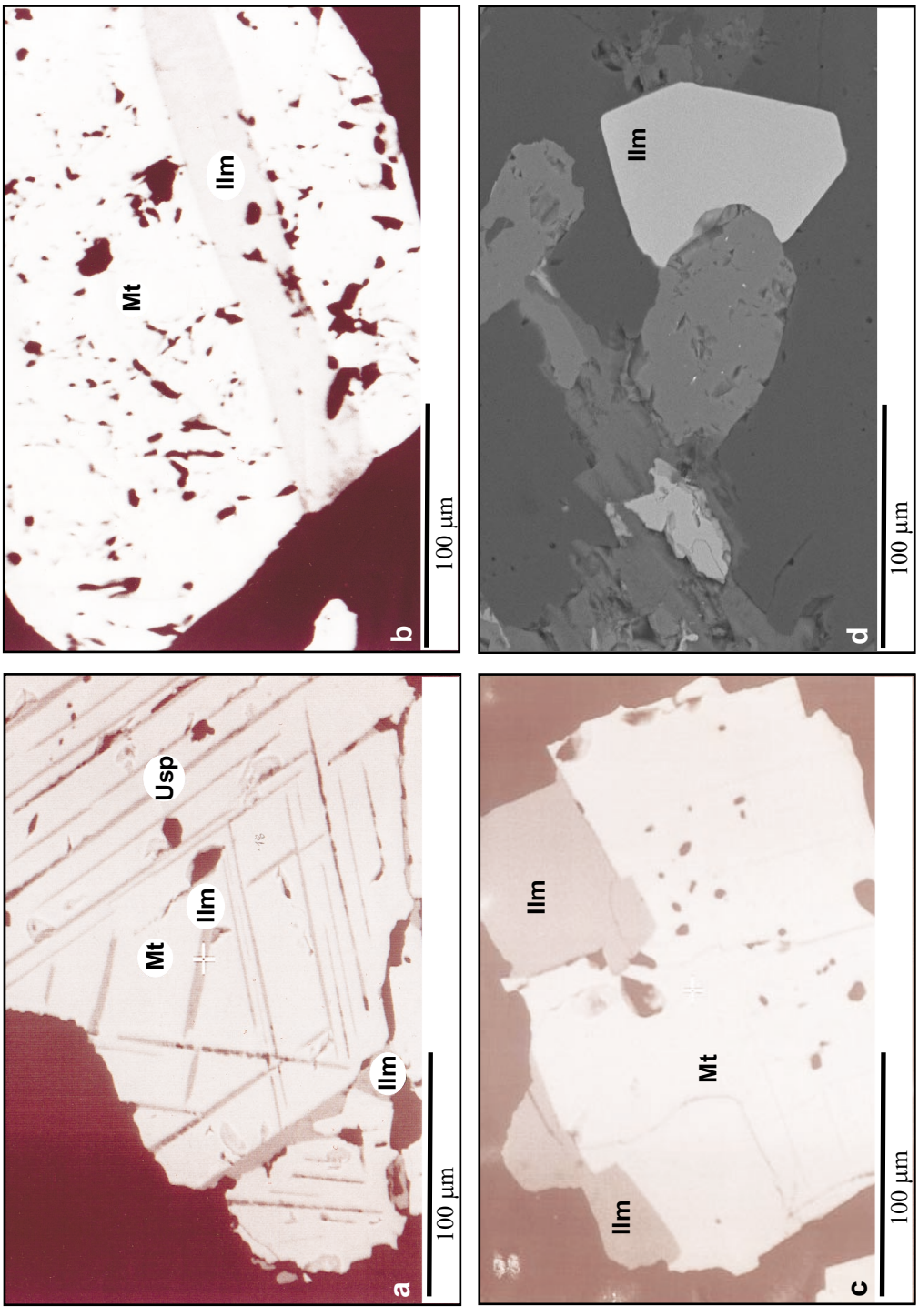

Figure 4. (a–d) Back-scattered electron (BSE) images showing specific forms of the iron-titanium oxides. In terms of magnetite (Mt), ulvöspinel (Usp) and ilmenite (Ilm).

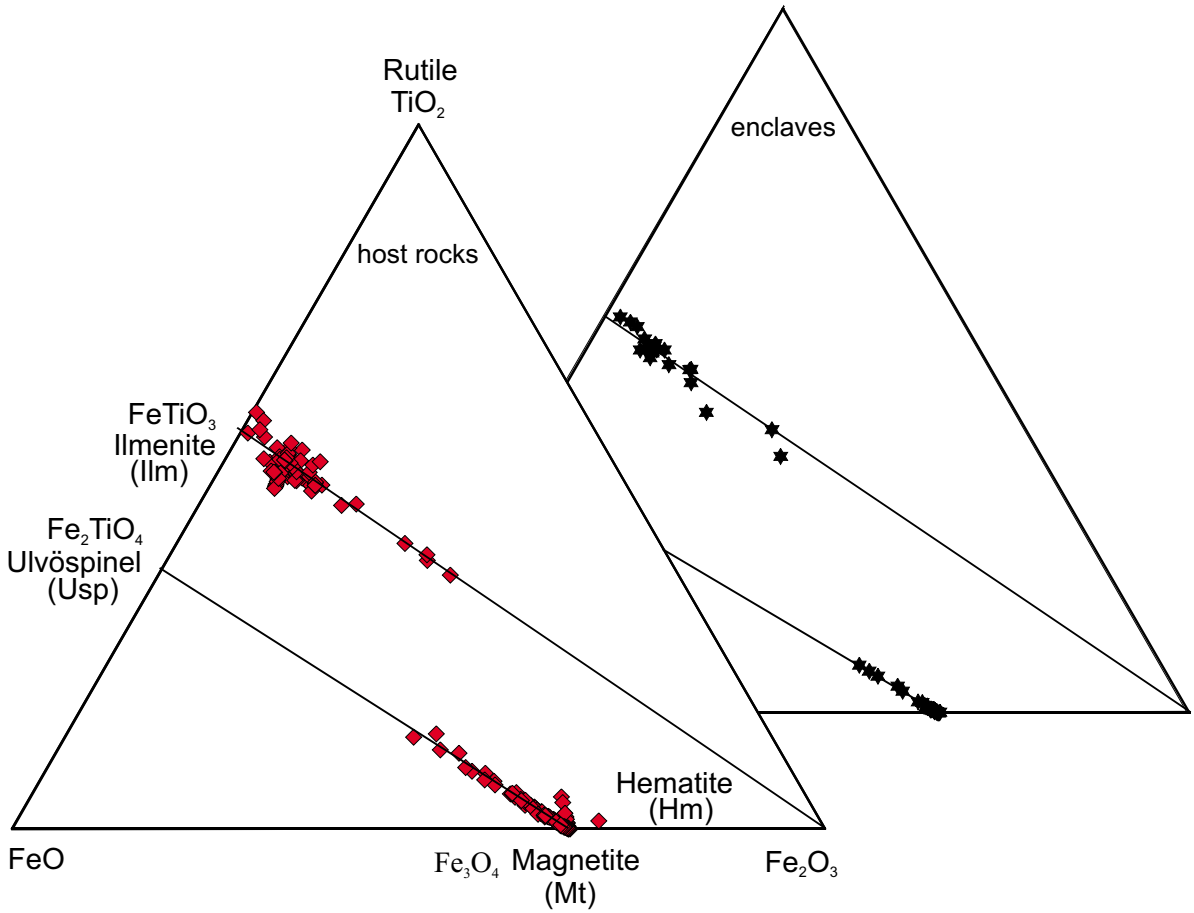

Figure 5. Nomenculature of the studied iron-titanium oxide of host rocks and MMEs.

forms, averaging 12.43 wt%. Chemical analyses show that the iron-titanium oxide forms in both host rocks and MMEs are compositionally very similar (Table 1).

The most common substitution is the $Ti^{4+} \Leftrightarrow Fe^{3+}$ in titanomagnetite in both host rocks and MMEs (Figure 6a, b). The rim to rim profiles for the titanomagnetites from the host rock and MMEs show that Ti^{4+} slowly decreases rimward and Fe^{3+} increases rimward (Figure 6a, b). Such variation can be attributed to a crystallization process that occurred at thermal equilibrium after magma interaction in dynamic magma systems (e.g., Nakamura 1995; Devine *et al.* 2003).

Geothermometry and Oxygen Barometry

The Fe-Ti oxide geothermometry and oxygen barometry are dependent on thermodynamic formulation based on a solution model (e.g., Spencer & Lindsley 1981). The frame of geothermometry and oxygen barometry must also be consistent with variation in the composition of coexisting Fe-Ti oxide minerals, namely titanomagnetite and ilmenite. In this study, Fe-Ti oxide geothermometry/oxygen barometry was used, based on the exchange reaction of Fe_3O_4 (Mt) + $FeTiO_3$ (Ilm) = Fe_2TiO_4 (Usp) + Fe_2O_3 (Hm), proposed by Spencer & Lindsley (1981). We focus on geothermometric and oxygen barometric calculations for coexisting titanomagnetite and ilmenite pairs from both host rocks and MMEs for all modal compositions of the plutons. The crystallization temperature and oxygen fugacity estimations for the host rocks were calculated from both titanomagnetite-ilmenite lamellae and titanomagnetite-ilmenite crystal pairs. Those for enclaves were estimated from adjacent titanomagnetite-ilmenite crystal pairs because of the lack of ilmenite lamellae in the titanomagnetite. Estimates of temperature and oxygen

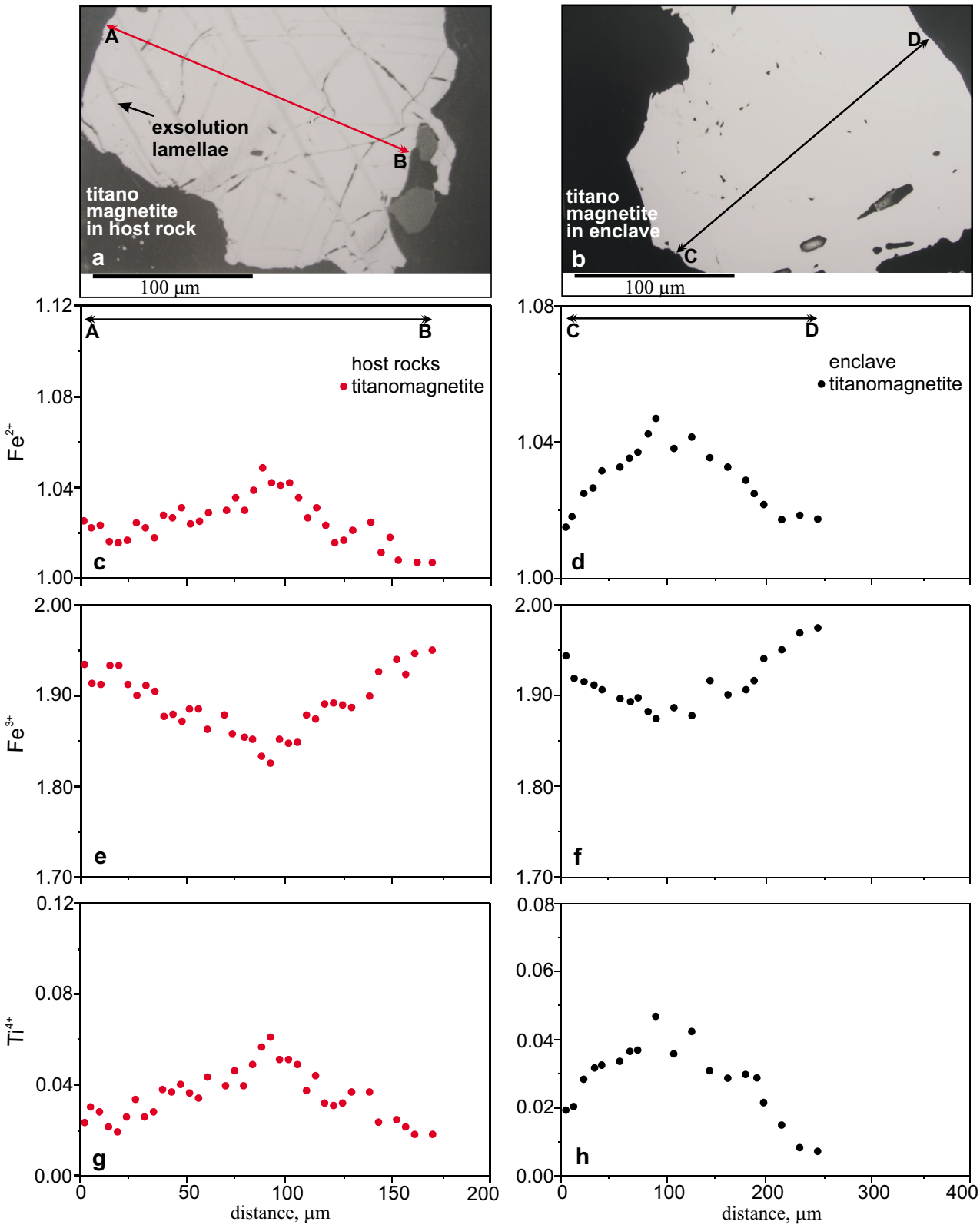

Figure 6. Ti^{4+}, Fe^{2+} and Fe^{3+} profiles of the titanomagnetites from the host rocks and MMEs.

fugacity range from logfO_2 of -15.30 to -20.48 for host rocks, logfO_2 of -15.39 to -20.80 for the MMEs and 617±6 to 758±23 °C in the host rocks, 622±6 to 735±24 °C in the MMEs, possibly indicating crystallization temperature (Figure 7 and Table 2). The estimates are consistent with logfO_2 and temperature values estimated by Karslı (2002) using the equation of Huebner & Sato (1970) for biotite composition and equation of Blundy & Holland (1990) for plagioclase-magnesio-hornblende compositions. The crystallization temperature and oxygen fugacity for titanomagnetite-ilmenite lamella pairs are lower than those for titanomagnetite-ilmenite crystal pairs. A good positive correlation has been observed between crystallization temperature and oxygen fugacities that are obtained from Fe-Ti oxides pairs (Figure 7). Ilmenite exsolution lamellae in the titanomagnetite formation temperatures are estimated between 651±9 and 740±21 °C by using titanomagnetite-ilmenite lamella pairs.

Discussion and Conclusions

The titanomagnetite, including cloth-textured exsolution lamellae with mostly tapered terminations, are common in the host rocks of the plutons compared to ther mafic microgranular enclaves. Titanomagnetite of the mafic microgranular enclaves never exsolves lamellae (Figure 3d). Yet the crystallization temperature and oxygen fugacity of the host rocks and their mafic microgranular enclaves are very similar. The estimates given here are

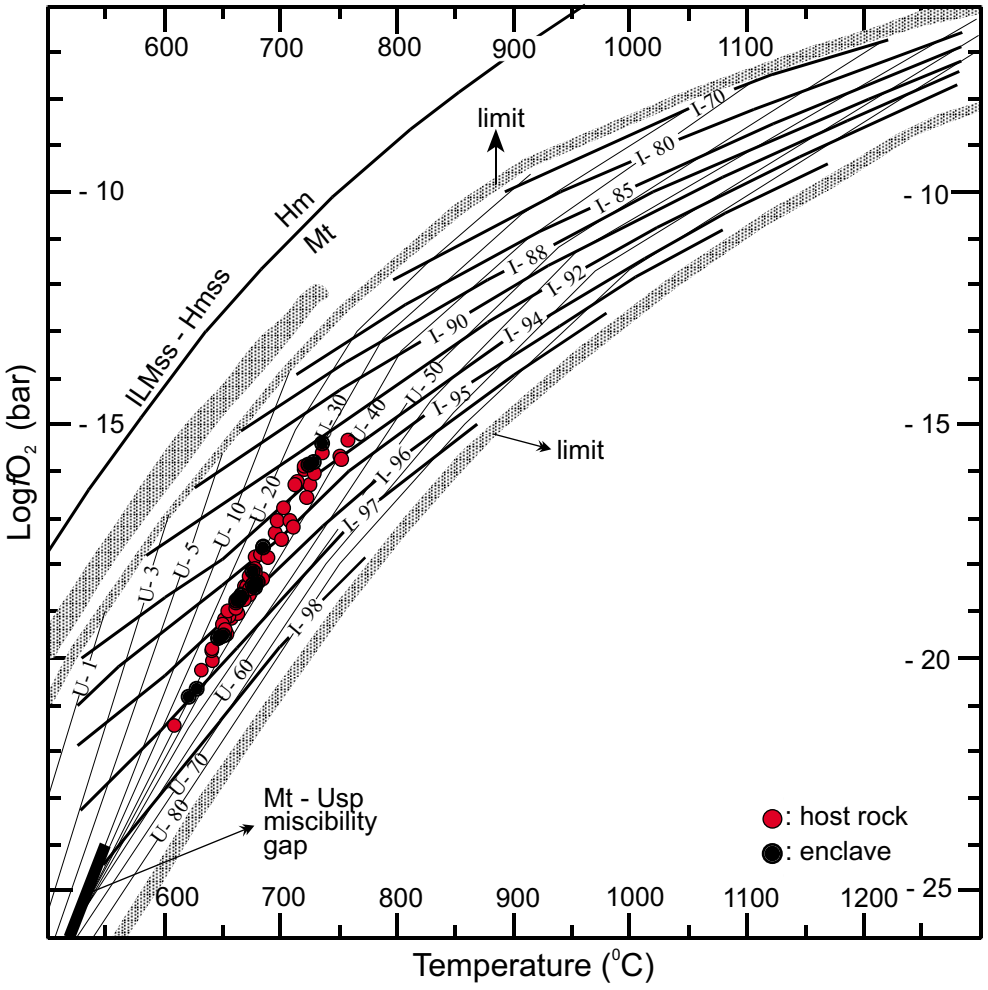

Figure 7. The plot of the investigated iron-titanium oxide on T-fO_2 grid for coexisting Mtss-Ilmss pairs, based on the solution model suggested by Spencer & Lindsley (1981). Mtss– Magnetite solid solution, Ilmss– Ilmenite solid solution, Hmss– Hematite solid solution.

Table 2. The temperature and oxygen fugacity values calculated from the iron-titanium oxides.

Host rocks (Dölek and Sarıçiçek Plutons)					
Sample-Pairs	Rock type-Pairs	a_{ulvo}	a_{ilm}	Temperature (°C)	LogfO_2 (bar)
D20-1 (46-50)	quartz monzonite/crystal	0.33	0.034	655 ± 10	-19.51
D20-2 (47-51)	quartz monzonite/crystal	0.30	0.036	649 ± 7	-19.53
D20-3 (53-55)	quartz monzonite/crystal	0.31	0.036	651 ± 9	-19.52
D20-4 (56-57)	quartz monzonite/crystal	0.31	0.033	642 ± 8	-20.01
D20-5 (49-52)	quartz monzonite/crystal	0.31	0.036	651 ± 9	-19.52
D12-1 (37-44)	granodiorite/crystal	0.29	0.044	674 ± 12	-18.45
D12-2 (38-43)	granodiorite/crystal	0.29	0.045	676 ± 16	-18.43
D12-3 (39-42)	granodiorite/crystal	0.27	0.050	680 ± 18	-17.86
D12-4 (40-45)	granodiorite/(ilmenite-lamellae)	0.29	0.050	685 ± 19	-17.78
Sr2-1 (22-30)	granodiorite/(ilmenit-lamellae)	0.32	0.38	666 ± 07	-19.18
Be-öz-1 (23-24)	granodiorite/crystal	0.29	0.053	687 ± 18	-17.65
Be-öz-2 (26-27)	granodiorite/crystal	0.29	0.045	676 ± 16	-18.43
Be-öz-3 (29-32)	granodiorite/(ilmenite-lamellae)	0.30	0.038	664 ± 10	-19.18
Be-öz-4 (30-31)	granodiorite/crystal	0.30	0.038	664 ± 10	-19.18
Is1-1 (2-3)	granodiorite/crystal	0.30	0.042	670 ± 15	-18.95
Is1-2 (4-5)	granodiorite/crystal	0.31	0.046	679 ±17	-18.18
Is1-3 (6-5)	granodiorite/(ilmenite-lamellae)	0.31	0.038	665 ± 11	-19.19
Is1-4 (7-10)	granodiorite/(ilmenite-lamellae)	0.32	0.038	666 ± 11	-19.18
Is1-5 (12-13)	granodiorite/crystal	0.31	0.046	679 ± 17	-18.18
Is1-6 (11-14)	granodiorite/crystal	0.32	0.041	668 ± 14	-18.75
Is1-7 (15-14)	granodiorite/(ilmenite-lamellae)	0.32	0.053	693 ± 19	-17.38
Ed14-1 (7-8)	granodiorite/(ilmenite-lamellae)	0.30	0.044	675 ± 15	-18.44
Ed14-2 (9-10)	granodiorite/(ilmenite-lamellae)	0.30	0.043	674 ± 15	-18.45
Ed14-3 (14-15)	granodiorite/crystal	0.29	0.040	658 ± 10	-18.91
Sr11-1 (4-5)	granite/crystal	0.30	0.037	651 ± 8	-19.48
Sr11-2 (6-8)	granite/crystal	0.29	0.026	617 ± 6	-20.48
Sç12-1 (39-36)	granite/(ilmenite-lamellae)	0.32	0.072	740 ± 21	-15.58
Sr20-1 (33-34)	granite/crystal	0.29	0.056	698 ± 20	-17.01
Sr20-2 (32-35)	granite/crystal	0.29	0.062	715 ± 20	-16.25
Sek5-1 (5-6)	granite/(ilmenite-lamellae)	0.33	0.046	680 ± 18	-17.81
Ah1-1 (23-24)	granite/(ilmenite-lamellae)	0.27	0.040	651 ± 9	-19.08
Ah1-2 (25-26)	granite/(ilmenite-lamellae)	0.27	0.041	653 ± 9	-19.01
Ah1-3 (27-28)	granite/(ilmenite-lamellae)	0.27	0.041	653 ± 9	-19.01
E25-1 (16-18)	quartz monzodiorite/crystal	0.29	0.067	722 ± 20	-15.95
E25-2 (17-19)	quartz monzodiorite/crystal	0.34	0.059	725 ± 20	-16.30
E25-3 (27-28)	quartz monzodiorite/crystal	0.29	0.058	702 ± 19	-16.80
E25-4 (55-54)	quartz monzodiorite/crystal	0.29	0.068	723 ± 22	-15.99
E25-5 (59-56)	quartz monzodiorite/crystal	0.40	0.068	758 ± 23	-15.30
E25-6 (63-64)	quartz monzodiorite/(ilm-lam.)	0.29	0.038	650 ± 7	-19.30
E25-7 (65-66)	quartz monzodiorite/(ilm-lam.)	0.29	0.062	715 ± 19	-16.25
Ah2-1 (2-3)	quartz monzodiorite/crystal	0.35	0.054	723 ± 22	-16.52
Ah2-2 (4-5)	quartz monzodiorite/crystal	0.34	0.052	709 ± 19	-17.01
Ah2-3 (6-4)	quartz monzodiorite/(ilm-lam.)	0.34	0.049	700 ± 19	-17.50
Ah2-4 (7-8)	quartz monzodiorite/crystal	0.37	0.050	710 ± 20	-17.13
Id2a-1 (7-8)	quartz monzodiorite/crystal	0.30	0.040	669 ± 13	-18.87
Id2a-2 (9-10)	quartz monzodiorite/crystal	0.32	0.041	670 ± 15	-18.65
Id2a-3 (11-12)	quartz monzodiorite/crystal	0.37	0.041	685 ± 19	-18.29

Table 2. (Continued)

Host rocks (Dölek and Sarıçiçek Plutons)					
Sample-Pairs	Rock name-Pairs	a_{ulvo}	a_{ilm}	Temperature (°C)	LogfO_2 (bar)
Id2a-4 (13-14)	quartz monzodiorite/crystal	0.30	0.042	671 ± 15	-18.95
Id4-1 (6-9)	quartz monzodiorite/crystal	0.29	0.041	670 ± 15	-18.96
Id4-2 (8-9)	quartz monzodiorite/crystal	0.29	0.034	644 ± 7	-19.81
Id4-3 (7-10)	quartz monzodiorite/crystal	0.29	0.046	680 ± 18	-18.39
Is4-1 (4-5)	quartz monzodiorite/(ilm-lam.)	0.29	0.047	682 ± 19	-18.10
Is4-2 (6-3)	quartz monzodiorite/(ilm-lam.)	0.31	0.040	670 ± 15	-18.70
Is4-3 (17-18)	quartz monzodiorite/crystal	0.29	0.43	660 ± 11	-18.77
Is4-4 (19-20)	quartz monzodiorite/crystal	0.30	0.042	671 ± 15	-18.95
Is4-5 (21-22)	quartz monzodiorite/crystal	0.34	0.042	667 ± 12	-18.50
Id17-1 (1-2)	quartz monzodiorite/crystal	0.29	0.035	646 ± 8	-19.79
Id17-2 (3-4)	quartz monzodiorite/crystal	0.29	0.043	660 ± 11	-18.77
Id17-3 (9-10)	quartz monzodiorite/crystal	0.29	0.033	630 ± 6	-20.25
Id17-4 (11-12)	quartz monzodiorite/crystal	0.30	0.47	684 ± 19	-18.27
Id11-2 (14-15)	quartz monzodiorite/(ilm-lam.)	0.32	0.061	720 ± 20	-16.02
Enclaves (Dölek and Sarıçiçek Plutons)					
Sample-Pairs	Rock name-Pairs	a_{ulvo}	a_{ilm}	Temperature (°C)	LogfO_2 (bar)
Id11*-1 (9-10)	monzodiorite/crystal	0.30	0.072	732 ± 23	-15.80
Id11*-2 (11-12)	monzodiorite/crystal	0.29	0.071	730 ± 23	-15.83
Is4*-1 (1-3)	quartz diorite/crystal	0.29	0.042	672 ± 15	-18.92
Is4*-2 (2-4)	quartz diorite/crystal	0.30	0.042	671 ± 15	-18.95
Is4*-3 (5-8)	quartz diorite/crystal	0.30	0.041	669 ± 14	-18.96
Is4*-4 (6-9)	quartz diorite/crystal	0.35	0.042	686 ± 18	-18.27
Is4*-5 (11-9)	quartz diorite/crystal	0.35	0.041	685 ± 19	-18.29
Is4*-6 (10-3)	quartz diorite/crystal	0.29	0.051	686 ± 19	-17.75
Id17*-1 (3-4)	diorite/crystal	0.29	0.047	683 ± 19	-18.19
Id17*-2 (5-8)	diorite/crystal	0.29	0.030	622 ± 6	-20.80
Id1c*-1 (20-22)	quartz monzodiorite/crystal	0.29	0.077	735 ± 24	-15.39
Is1*-1 (1-4)	quartz monzodiorite/crystal	0.30	0.031	630 ± 6	-20.52
Is1*-2 (2-3)	quartz monzodiorite/crystal	0.31	0.036	651 ± 9	-19.52
Is1*-3 (5-6)	quartz monzodiorite/crystal	0.33	0.042	675 ± 16	-18.52
Is1*-4 (7-8)	quartz monzodiorite/crystal	0.29	0.037	648 ± 9	-19.54

Note:a_{ilm}= 0.5 Fe^{3+}/ 0.5Fe^{3+} + Ti^{4+} + Fe^{2+}, a_{ulvo}= 2 Fe^{2+} Ti^{4+}/(2 Fe^{2+} +Ti^{4+}) + Fe^{2+} + 2 Fe^{3+}. T(°C) and LogfO_2 (bar) were obtained from the diagram proposed by Spencer & Lidsley (1981).

consistent with temperature and fugacity data from Aydın *et al.* (2003) and Karslı *et al.* (2007) using amphibole-plagioclase thermometry and biotite compositions for oxygen fugacity. Exsolution lamellae of ilmenite in titanomagnetite-titanomagnetite pairs have yielded about 679±18 °C, the probable temperature of formation of the exsolution lamellae and this value should reflect the hybridization temperature and/or thermal equilibrium between the felsic and mafic magmas along with their interaction process. Hence, felsic and mafic magma interactions play an important role in the petrogenesis of plutonic systems where mantle-derived mafic magma is injected into a crustal-derived felsic magma chamber (e.g., Wiebe 1980; Vernon 1984; Didier & Barbarin 1991; Barbarin & Didier 1992; Poli & Tommasini 1999; Perugini & Poli 2000). Karslı *et al.* (2007) proposed an

interaction model for mafic injection into the felsic magma chamber, based on the geochemical and isotopic properties of the plutons. In the injection model, thermal diffusion occurs between two contrasting magmas, when the cooler felsic magma and hotter mafic magma come into contact (e.g., Fernandez & Barbarin 1991). The hotter mafic magma quenches, but raises the temperature of the felsic magma. After the thermal exchange between felsic and mafic magmas, the felsic magma cools. Hence, injection of hotter basic magma periodically causes temperature fluctuation in a dynamic felsic magma chamber (Wiebe 1980; Fernandez & Barbarin 1991; Barbarin & Didier 1992).

As mentioned above, titanomagnetite and related early crystallizing phases are also envisaged as being temperature-sensitive (e.g., Price 1981; Sadıklar & Hanedan 1997; Venezky & Rutherford 1999; Harlov 2000; Devine *et al.* 2003). In addition, Nakamura (1995) explained that Fe-Ti oxide compositions were affected by serial injection of more mafic magma into the felsic magma chamber. Sadıklar & Hanedan (1997) experimentally showed that exsolution textures such as cloth-texture formed by remelting of the titanomagnetites in the rhyolitic rocks, and that texture indicates a compositional adjustment of titanomagnetite at higher temperature. Devine *et al.* (2003) proposed that Ti rimward diffusion in titanomagnetite is sensitive to temperature fluctuation caused by magma interaction. A possible cause of exsolution lamellae in titanomagnetite in the studied granitoid systems is reheating of the crystals, caused by injection of more mafic magma into the felsic chamber. During this process, some early-formed titanomagnetite crystals cannot remain stable and then partially decompose and homogenize. Remaining titanomagnetite then reaches equilibrium with the host melt at higher temperatures. Thus, temperature fluctuation can result in an exsolution texture dependent on temperature criteria in dynamic magma system. The lack of lamellae in titanomagnetite from the MMEs in the studied plutons is because the mafic melt was initially hotter than the felsic melt. Also, the similarities in temperature and $\log fO_2$ in both host rocks and MMEs may be expected in coeval felsic and mafic magma interaction in dynamic magma sytems (e.g., Holden *et al.* 1991; Elburg 1996; Perugini & Poli 2000). This is particularly so in the studied plutons, suggesting hybridization in their genesis and that both magmas reached thermal equilibrium and then crystallized after interaction of crustal-derived more felsic and mantle-derived more mafic magmas during crystallization of the plutons. A Ti^{4+} rimward decrease and Fe^{3+} rimward increase in titanomagnetites also provides supporting evidence for magma interactions in the genesis of the Dölek and Sarıçiçek plutons.

Overall data and mineral chemistry characteristics suggest a mixing model in the formation of the studied plutons. But, in what geodynamic model do coeval magmas occur and mix? A popular model holds that underplating is a well-known mechanism responsible for genesis of the hybrid plutons. In the Eastern Pontides, Late Cretaceous volcanic arc magmatism was attributed to northward subduction of the northern branch of Neotethys (Şengör & Yılmaz 1981; Okay & Şahintürk 1997). The collision between the Pontides and the Anatolide-Tauride block is dated as Early Paleocene (Okay *et al.* 1997). But, to mix coeval magmas derived a lithospheric upper mantle (mafic end-member) and from the lower crust (felsic end-member), a thermal anomaly is needed. Upwelling of hot asthenospheric material in response to an extensional regime results in thermal perturbation and this thermal activity may initiate melting of the lithospheric mantle. Then, the intrusion of hot lithospheric mantle-derived mafic magma may induce the melting of the lower crust. Extensive interaction between the lower crust-derived melt and lithospheric mantle-derived magma produced the hybrid plutons in a post-collisional extensional tectonic setting during the Eocene in the Eastern Pontides.

Acknowledgements

This study was supported by the Research Foundation of Karadeniz Technical University. Orhan Karslı is most grateful to his hosts at the Mineralogy Institute in Heidelberg during his DAAD scholarship. In particular, we would like to thank Rainer Altherr and Hans-Peter Meyer for permission to use the microprobe in their laboratory. Sincere thanks are given to M. Cemal Göncüoğlu for his constructive comments on an earlier version of the manuscript. Reviewers Durmuş Boztuğ and Sibel Tatar are thanked for their thoughtful comments and helpful suggestions that improved the manuscript. Editorial comments by Erdin Bozkurt are also acknowledged. Raif Kandemir is thanked for his never-ending assistance during field work. John A. Winchester edited English of the final text.

References

AKIN, H. 1979. Geologie, magmatismus und Lagerstattenbildung im ostpontischen Gebirge/Türkei aus der Sicht der Plattentektonik. *Geolgische Rundschau* **68**, 253–283.

ANDERSEN, D.J., BISHOP, F.C. & LINDSLEY, D.H. 1991. Internally consistent solution models for Fe-Mg-Mn-Ti oxides: Fe-Mg-Ti oxides and olivine. *American Mineralogist* **76**, 427–444.

AYDIN, F., KARSLI, O. & SADIKLAR, M.B. 2003. Mineralogy and chemistry of biotites from eastern Pontide granitoid rocks, NE Turkey: Some petrological implications for granitoid magmas. *Chemie der Erde-Geochemistry* **63**, 163–182.

BARBARIN, B. & DIDIER, J. 1992. Genesis and evolution of mafic microgranular enclaves through various types of interaction between coexisting felsic and mafic magmas. *Transactions of the Royal Society of Edinburgh, Earth Science* **83**, 145–153.

BLUNDY, J.D. & HOLLAND, T.J.B. 1990. Calcic amphibole equilibria and a new amphibole-plagioclase geothermometer. *Contributions to Mineralogy and Petrology* **104**, 208–224.

BOZTUĞ, D., JONCKHEERE, R., WAGNER, G.A. & YEĞİNGİL, Z. 2004. Slow Senonian and fast Paleocene–Early Eocene uplift of the granitoids in the central eastern Pontides, Turkey: Apatite fission-track results. *Tectonophysics* **382**, 213–228.

BOZTUĞ, D., ERÇİN, A.I., KURUÇELİK, M.K., GÖÇ, D., KÖMÜR, I. & İSKENDEROĞLU, A. 2006. Main geochemical characteristics of the composite Kaçkar batholith derived from the subduction through collision to extentional stages of Neo-Tethyan convergence system in the Eastern Pontides, Turkey. *Journal of Asian Earth Sciences* **27**, 286–302.

BOZTUĞ, D. & HARLAVAN, Y. 2007. K-Ar ages of granitoids unravel the stages of Neo-tethyan convergence in the eastern Pontides and central Anatolia, Turkey. *International Journal of Earth Sciences*, doi:10.1007/s00531-007-0176-0.

BOZTUĞ, D., JONCKHEERE, R., WAGNER, G.A., ERÇİN, A.I. & YEĞİNGİL, Z. 2007. Titanite and zircon fission-track dating resolves successive igneous episodes in the formation of the composite Kaçkar batholith in the Turkish eastern Pontides. *International Journal of Earth Science* **96**, 875–886.

DEVINE, J.D., RUTHERFORD, M.J., NORTON, G.E. & YOUNG, S.R. 2003. Magma storage region processes inferred from geochemistry of Fe-Ti oxides in andesitic magma, Soufriere Hills Volcano, Montserrat, W.I. *Journal of Petrology* **44**, 1375–1400.

DIDIER, J. & BARBARIN, B. 1991. Review of the main hypotheses proposed for the genesis and evoluation of mafic microgranular enclaves. *In:* DIDIER, J. & BARBARIN, B. (eds), *Enclaves and Granite Petrology, Developments in Petrology*. Amsterdam **13**, 367–373.

DOKUZ, A., TANYOLU, E. & GENÇ, S. 2006. A mantle- and a lower crust-derived bimodal suite in the Yusufeli (Artvin) area, NE Turkey: trace element and REE evidence for subduction-related rift origin of Early Jurassic Demirkent intrusive complex. *International Jounal of Earth Sciences* **95**, 370–394.

ELBURG, M.A. 1996. Evidence of isotopic equilibration between microgranitoid enclaves and host granodiorite, Warburton Granodiorite, Lachlan Fold Belt, Australia. *Lithos* **38**, 1–22.

FERNANDEZ, A.N. & BARBARIN, B. 1991. Relative rheology of coexisting mafic and felsic magmas: Nature of resulting interaction processes. Shape and mineral fabrics of mafic microgranular enclaves. *In:* DIDIER, J. & BARBARIN, B. (eds), *Enclaves and Granite Petrology, Developments in Petrology*. Amsterdam **13**, 263–275.

FROST, B.R. & LINDSLEY, D.H. 1991. The occurrence of iron-titanium oxides in igneous rocks. *In:* LINDSLEY, D.H. (ed), *Oxide Minerals: Petrologic and Magnetic Significance*. Reviews in Mineralogy, Mineralogical Society of America, Washington **25**, 433–468.

FROST, B.R., LINDSLEY, D.H. & ANDERSEN, D.J. 1988. Fe-Ti oxide-silicate equilibria: Assemblages with fayalitic olivine. *American Mineralogist* **73**, 727–740.

FROST, B.R. & MAHOOD, G.A. 1987. Field, chemical and physical constraints on mafic-felsic interaction in the Lamarck granodiorite, Sierra Nevada, California. *Geological Society of America Bulletin* **99**, 272–291.

GEDİK, A., ERCAN, T., KORKMAZ, S. & KARATAŞ, S. 1992. Rize-Fındıklı-Çamlihemşin arasında (Doğu Karadeniz) yer alan magmatik kayaçların petrolojisi ve Doğu Pontidlerdeki bölgesel yayılımları [Petrology of the magmatic rocks around Rize-Fmdıklı-Çamlıhemşin (Eastern Black Sea) and their distribution at the Eastern Pontides]. *Geological Bulletin of Turkey* **35**, 15–38 [in Turkish with English abstract].

GHIORSO, M.S. & SACK, R.O. 1991. Fe-Ti oxide geothermometry: thermodynamic formulation and the estimation of intensive variables in silicic magmas. *Contributions to Mineralogy and Petrology* **108**, 485–510.

HAGGERTY, S.E. 1991. Oxide textures-a mini atlas. *In:* LINDSLEY, D.H. (ed), *Oxide Minerals: Petrologic and Magnetic Significance*. Reviews in Mineralogy, Mineralogical Society of America, Washington **25**, 129–219.

HAMMOND, P.A. & TAYLOR, L.A. 1982. The ilmenite/titano-magnetite assemblage: Kinetics of re-equilibration. *Earth and Planetary Science Letters* **61**, 143–150.

HARLOV, D.H. 1992. Comparative oxygen barometry in granulites, Bamble sector, SE Norway. *Journal of Geology* **100**, 447–464.

HARLOV, D.E. 2000. Titaniferous magnetite-ilmenite thermometry and titaniferous magnetite-ilmenite-orthopyroxene-quartz oxygen barometry in granulite facies gneisses, Bamble Sector, SE Noway: Implications for the role of high-grade CO_2-rich fluids during granulite genesis. *Contributions to Mineralogy and Petrology* **1139**, 180–197.

HUEBNER, J.S. & SATO, M. 1970. The oxygen fugacity-temperature relationships of manganese oxide and nickel oxide buffers. *American Mineralogist* **55**, 934–952.

HIBBARD, M.J. 1991. Textural anatomy of twelve magma-mixed granitoid systems. *In:* DIDIER, J. & BARBARIN, B. (eds), *Enclaves and Granite Petrology, Developments in Petrology*. Amsterdam **13**, 431–444.

HOLDEN, P., HALLIDAY, A.N., STEPHENS, W.E. & HENNEY, P.J. 1991. Chemical and isotopic evidence for major mass transfer between mafic enclaves and felsic magma. *Chemical Geology* **92**, 135–152.

KARSLI, O., AYDIN, F. & SADIKLAR, M.B. 2002. Geothermobarometric investigation of the Zigana Granitoid, eastern Pontides, Turkey. *International Geology Review* **44**, 277–286.

KARSLI, O. 2002. *Granitoyid Kayaçlarda Magma Etkileşimleri İçin Petrografik, Mineralojik ve Kimyasal Bulgular: Dölek ve Sariçiçek Plutonları (Gümüşhane, KD-Türkiye) [Petrographic, Mineralogic and Chemical Evidence for Magma Interaction in Granitoid Rocks: Dölek and Sarıçiçek Plutons (Gümüşhane, NE Turkey)]*. PhD Thesis, Karadeniz Technical University, Trabzon, Turkey [in Turkish with English abstract, unpublished].

KARSLI, O., AYDIN, F. & SADIKLAR, M.B. 2004a. Magma interaction recorded in plagioclase zoning in granitoid systems, Zigana Granitoid, Eastern Pontides, Turkey. *Turkish Journal of Earth Sciences* **13**, 287–305.

KARSLI, O., AYDIN, F. & SADIKLAR, M.B. 2004b. The morphology and chemistry of K-feldspar megacrysts from İkizdere Pluton: evidence for acid and basic magma interactions in granitoid rocks, NE Turkey. *Chemie der Erde-Geochemistry* **64**, 155–170.

KARSLI, O., CHEN, B., AYDIN, F. & ŞEN, C. 2007. Geochemical and Sr-Nd-Pb isotopic compositions of the Eocene Dölek and Sarıçiçek Plutons, Eastern Turkey: Implications for magma interaction in the genesis of high-K calc-alkaline granitoids in a post-collision extensional setting. *Lithos* **98**, 67–96.

KUMAR, S., RINO, V. & PAL, A.B. 2004. Field evidence of magma mixing from microgranular enclaves hosted in Palaeoproterozoic Malanjkhand granitoids, Central India. *Gondwana Research* **7**, 539–548.

LINDSLEY, D.H. 1981. Some experiment pertaining to the magnetite-ulvöspinel miscibility gap. *American Mineralogist* **66**, 759–762.

LINDSLEY, D.H., FROST, B.R., ANDERSEN, D.J. & DAVIDSON, P.M. 1990. Fe-Ti oxide-silicate equilibria: assemblages with orthopyroxene. *In:* SPENCER, R.J. & CHOU, I.M. (eds), *Fluid-mineral Interactions: A Tribute to EUGSTER H.P.* The Geochemical Society Publication **2**, 103–119.

MOORE, W.J., MCKEE, E.H. & AKINCI, Ö. 1980. Chemistry and chronology of plutonic rocks in the Pontide Mountains, Northern Turkey. *Symposium of European Copper Deposit*, Belgrade, 209–216.

NAKAMURA, M. 1995. Continious mixing of crystal mush and replenished magma in the ongoing Unzen eruption. *Geology* **23**, 807–810.

OKAY, A.I. & ŞAHİNTÜRK, Ö. 1997. Geology of the Eastern Pontides. *In:* ROBINSON, A.G. (ed), *Regional and Petroleum Geology of the Black Sea and Surrounding Region*. American Association Petroleum Geologist Memoir **68**, 291–310.

OKAY, A.İ., ŞAHİNTÜRK, Ö. & YAKAR, H. 1997. Stratigraphy and tectonics of the Pulur (Bayburt) region in the Eastern Pontides. *Mineral Research and Exploration Institute (MTA) of Turkey Bulletin* **119**, 1–24.

PERUGINI, D. & POLI, G. 2000. Chaotic dynamics and fractals in magmatic interaction processes: A different approach to the interpretation of mafic microgranular enclaves. *Earth and Planetary Science Letters* **175**, 93–103.

PERUGINI, D., POLI, G., CHRISTOFIDES, G. & ELEFTHERIADIS, G. 2003. Magma mixing in the Sithonia Plutonic Complex, Greece: evidence from mafic microgranular enclaves. *Mineralogy and Petrology* **78**, 173–200.

PERUGINI, D., VENTURA, G., PETRELLI, M. & POLI, G. 2004. Kinematic significance of morphological structures generated by mixing of magmas: a case study from Salina Island (southern Italy). *Earth and Planetary Science Letters* **222**, 1051–1066.

POLI, G.E. & TOMMASINI, S. 1991. Model for the origin and significance of microgranular enclaves in calc-alkaline granitoids. *Journal Petrology* **32**, 657–666.

POLI, G.E. & TOMMASINI, S. 1999. Geochemical modelling of acid-basic magma interaction in the Sardinia-Corsica Batholith: The case study of Sarrabus, Southeastern Sardinia, Italy. *Lithos* **46**, 553–571.

POUCHOU, J.L. & PICHOIR, F. 1985. 'PAP' (ø.ρ.Z) correction procedure for improved quantitative microanalysis. *In:* ARMSTRONG, J.T. (ed), *Microbeam Analysis*. San Francisco Press 104–106.

PRICE, G.D. 1981. Subsolidus phase relations in the titanomagnetite solid solution series. *American Mineralogist* **66**, 751–758.

ROBINSON, A.G., BANKS, C.J., RUTHERFORD, M.M. & HIRST, J.P.P. 1995. Stratigraphic and structural development of the Eastern Pontides, Turkey. *Journal of the Geological Society, London* **152**, 861–872.

SADIKLAR, M.B. & HANEDAN, A. 1997. Entmischte Magnetite in Obsidian (Ikizdere/NE-Turkei) und deren Genetische Bedeutung. *Beihefte zum European Journal of Mineralogy* **9**, p. 301.

ŞAHİN, S.Y., GÜNGÖR, Y. & BOZTUĞ, D. 2004. Comparative petrogenetic investigation of composite Kaçkar Batholith granitoids in Eastern Pontide magmatic arc-Northern Turkey. *Earth Planets and Space* **56**, 429–446.

ŞEN, C., ARSLAN, M. & VAN, A. 1998. Geochemical and petrological characteristics of the Eastern Pontide Eocene (?) alkaline volcanic province, NE Turkey. *Turkish Journal of Earth Sciences* **7**, 231–239.

ŞENGÖR, A.M.C. & YILMAZ, Y. 1981. Tethyan evolution of Turkey: a plate tectonic approach. *Tectonophysics* **75**, 181–241.

ŞENGÖR, A.M.C., ÖZEREN, S., GENÇ, T. & ZOR, E. 2003. East Anatolian high plateau as a mantle-supported, north-south shortened domal structure. *Geophysical Research Letters* **30 (24)**, 8044, doi:10.1029/2003GL018192.

SPENCER, K.J. & LINDSLEY, D.H. 1981. A solution model for coexisting iron-titanium oxides. *American Mineralogist* **66**, 1189–1201.

TANER, M.F. 1977. *Etude géologique et petrographique de la region de Güneyce-İkizdere, située au sud de Rize (Pontides orientalas, Turquie)*. PhD Thesis, Université de Geneve, Switzerland [unpublished].

TOKEL, S. 1977. Eocene calc-alkaline andesites and geotectonism in the Eastern Black Sea region. *Geological Bulletin of Turkey* **20**, 49–54 [in Turkish with English abstract].

TOPUZ, G., ALTHERR, R., SCHWARZ, W.H., SIEBEL, W., SATIR, M. & DOKUZ, A. 2005. Post-collisional plutonism with adakite-like signatures: the Eocene Saraycık granodiorite (Eastern Pontides, Turkey). *Contributions to Mineralogy and Petrology* **150**, 441–455.

TOPUZ, G. & OKAY, A.İ. 2006. Comment on Petrography and petrology of the calc-alkaline Sarıhan Granitoid (NE-Turkey): An example of magma mingling and mixing. *Turkish Journal of Earth Sciences* **15**, 373–377.

VENEZKY, D.Y. & RUTHERFORD, M.J. 1999. Petrology and Fe-Ti oxide re-equilibration of the 1991 Mount Unzen mixed magma. *Journal of Volcanology and Geothermal Research* **89**, 213–230.

VERNON, R.H. 1984. Microgranitoid enclaves in granites-globules of hybrid magma quenched in a plotonic environment. *Nature* **309**, 438–439.

VERNON, R.H. 1990. Crystallization and hybridisation in microgranitoid enclave magmas: microstructural evidence. *Journal of Geophysical Research* **95**, 17849–17859.

WAIGHT, T.E., MAAS, R. & NICHOLLS, I.A. 2000. Fingerprinting feldspar phenocrysts using crystal isotopic composition stratigraphy: Implications for crystal and magma mingling in S-type granites. *Contributions to Mineralogy and Petrology* **139**, 227–239.

WIEBE, R.A. 1980. Commingling of contrasted magmas in the plutonic environment: Examples from The Nain Anorthositic Complex. *Journal of Geology* **88**, 197–209.

YILMAZ, Y. 1972. *Petrology and Structure of the Gümüşhane Granite and Surrounding Rocks, North-eastern Anatolia*. PhD Thesis, University of London, England [unpublished].

YILMAZ, S. & BOZTUĞ, D. 1996. Space and time relations of three plutonic phase in the eastern Pontides, Turkey. *International Geology Review* **38**, 935–956.

YILMAZ, Y., TÜYSÜZ, O., YİĞİTBAŞ, E., GENÇ, Ş.C. & ŞENGÖR, A.M.C. 1997. Geology and tectonic evolution of the Pontides. *In:* ROBINSON, A.G. (ed), *Regional and Petroleum Geology of the Black Sea and Surrounding Region*. American Association Petroleum Geologist Memoir **68**, 183–226.

YILMAZ, C. & KANDEMİR, R. 2006. Sedimentary records of the extensional tectonic regime with temporal cessation: Gümüşhane Mesozoic Basin (NE-Turkey). *Geologica Carpathica* **57**, 3–13.

Received 13 April 2006; revised typescript received 15 October 2007; accepted 07 December 2007